The role of bedrock topography on subsurface storm flow

Jim Freer,[1] J. J. McDonnell,[2] K. J. Beven,[1] N. E. Peters,[3] D. A. Burns,[1,4] R. P. Hooper,[3,5] B. Aulenbach,[3] and C. Kendall[6]

[1]   We conducted a detailed study of subsurface flow and water table response coupled with digital terrain analysis (DTA) of surface and subsurface features at the hillslope scale in Panola Mountain Research Watershed (PMRW), Georgia. Subsurface storm flow contributions of macropore and matrix flow in different sections along an artificial trench face were highly variable in terms of timing, peak flow, recession characteristics, and total flow volume. The trench flow characteristics showed linkages with the spatial tensiometer response defining water table development upslope. DTA of the ground surface did not capture the observed spatial patterns of trench flow or tensiometric response. However, bedrock surface topographic indices significantly improved the estimation of spatial variation of flow at the trench. Point-scale tensiometric data were also more highly correlated with the bedrock surface-based indices. These relationships were further assessed for temporal changes throughout a rainstorm. Linkages between the bedrock indices and the trench flow and spatial water table responses improved during the wetter periods of the rainstorm, when the hillslope became more hydrologically connected. Our results clearly demonstrate that in developing a conceptual framework for understanding the mechanisms of runoff generation, local bedrock topography may be highly significant at the hillslope scale in some catchments where the bedrock surface acts as a relatively impermeable boundary.   *INDEX TERMS:* 1860 Hydrology: Runoff and streamflow; 1866 Hydrology: Soil moisture; 1824 Hydrology: Geomorphology (1625); *KEYWORDS:* bedrock topography, subsurface storm flow, macropores, soil moisture, topographic index, trench flow

1. Introduction

[2]   In attempting to understand the mechanisms of catchment storm flow in a particular study catchment, the hydrologist is faced with many problems of complexity, heterogeneity and scale, the limitations of available measurement techniques, choice of measurement sites, and the uncontrolled variability of the sequence of inputs. Most problematic is how to relate field measurements made at several different scales so that they are meaningful for developing a perceptual or predictive model of the relevant processes controlling the response at the catchment scale (see, for example, the discussions of *Beven* [1989a, 2000] and *McDonnell* [1990]). This remains an open question because there are still processes, such as preferential flows in soil macropores, for which we do not have an accepted quantitative description. Also every catchment is unique and every experiment different so that observations may add much to the understanding of a particular site but only marginally to more general understanding of the modes of response of hillslopes and catchments. Extrapolating that knowledge to other, even nearby, hillslopes and catchments remains problematic.

[3]   Such extrapolation requires a model, preferably a model that is consistent with the spatial pattern of hydrological responses on the hillslopes. There is, as yet, no general agreement about an appropriate distributed model to use to predict hillslope hydrological responses; indeed the difficulties of constructing such a model have been the subject of considerable discussion [see *Beven*, 1989b, 1996a, 1996b, 2001; *Grayson et al.*, 1992; *Bronstert*, 1999]. One approach toward constructing a parsimonious model has been to base the predictions on indices of hydrological similarity based on topography and soils data [*Kirkby*, 1975; *Beven and Kirkby*, 1979; *O'Loughlin*, 1981; *Ambroise et al.*, 1996; *Iorgulescu and Musy*, 1997]. This study represents one of a number of recent efforts that have used spatially distributed field observations with a view to evaluating the similarity index approach to the prediction of hydrological responses [see *Burt and Butcher*, 1985; *Jones*, 1986; *Jordan*, 1994; *Barling et al.*, 1994; *Nyberg*, 1996; *Moore and Thompson*, 1996; *Crave and Gascuel-Odoux*, 1997; *Lamb et al.*, 1997]. None of these studies, however, has attempted to combine continuous subsurface flow measurements and spatial predictions of soil moisture coupled with detailed soil depth measurements in the assessment of spatial terrain indices.

[1]Department of Environmental Sciences, IENS, University of Lancaster, Lancaster, UK.
[2]Department of Forest Engineering, Oregon State University, Corvallis, Oregon, USA.
[3]U.S. Geological Survey, Atlanta, Georgia, USA.
[4]Now at U.S. Geological Survey, Troy, New York, USA.
[5]Now at U.S. Geological Survey, Northborough, Massachusetts, USA.
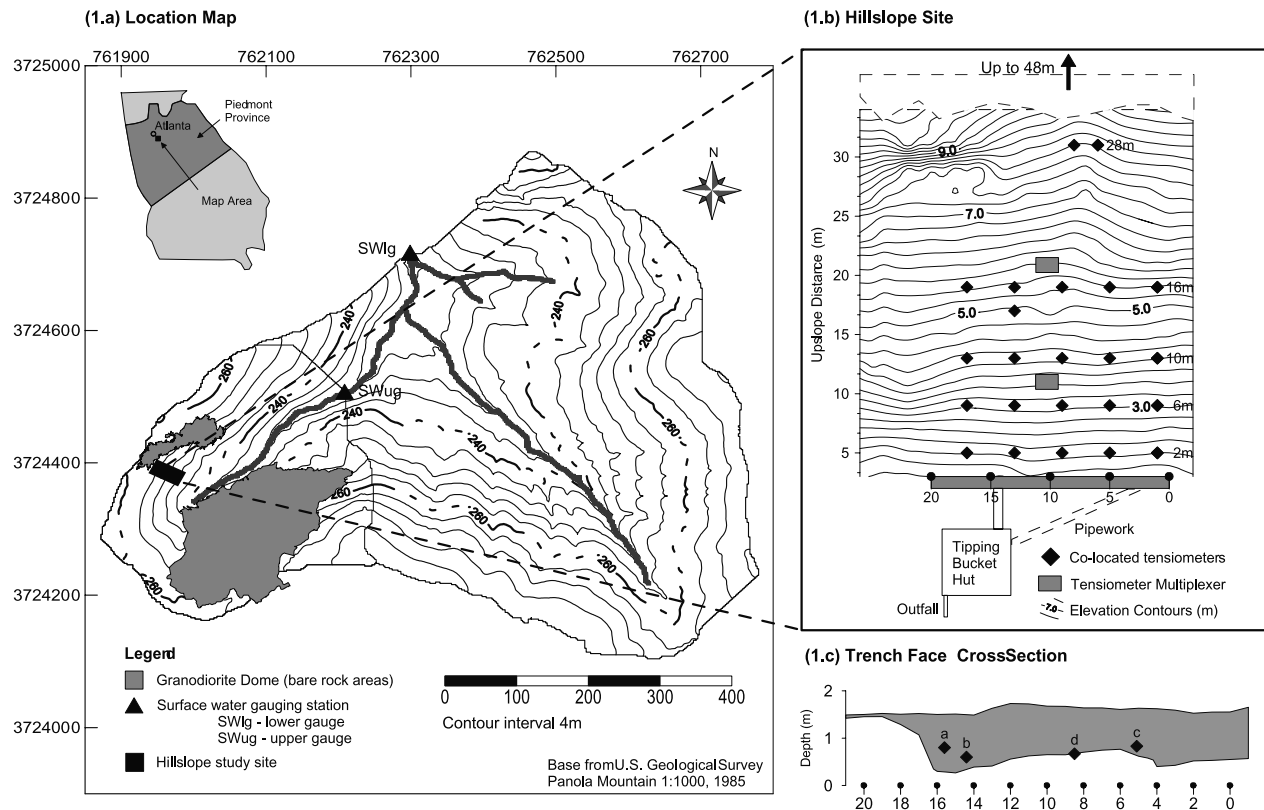[6]U.S. Geological Survey, Menlo Park, California, USA.

Figure 1. PMRW, the 10 ha subcatchment and the 20 × 48 m hillslope site.

[4] There is a long history of studies of hillslope hydrological responses that have attempted to use trenches and troughs to collect hillslope discharges, from the classic experiments of *Hewlett and Hibbert* [1963] and *Dunne and Black* [1970] onwards. A review of the early work is given by *Atkinson* [1978], who also points out the impacts of the trench itself on the flowlines and pathways (which can involve the formation of saturated wedges and variability in contributing areas due to flowline changes at the margins of the trench). Since that time there have been a number of interesting experiments based on the collection of near-surface downslope flows in troughs [e.g., *McDonnell*, 1990; *Turton et al.*, 1992; *Tsuboyama et al.*, 1994; *Woods and Rowe*, 1996; *Buttle and Turcotte*, 1999; *Hutchinson and Moore*, 2000] and there is also perhaps a greater appreciation that deeper pathways may be important in controlling hillslope contributions to the stream channel in many catchments [e.g., *Genereux et al.*, 1993; *Hinton et al.*, 1993].

[5] *Woods and Rowe* [1996] found that flow patterns along a 60 m trench face varied considerably with changing antecedent conditions and rainstorm characteristics. The flow variations were observed for accumulated trench flows between rainstorms and as a temporal sequence of snapshots during individual rainstorms. For larger rainstorms, the spatial variability of storm flow of combined trench flows was reduced by accounting for common surface topographic features (characterized by the upslope contributing areas). These results allowed *Woods and Rowe* [1996] to conclude that models could be developed that would predict the spatial variability in subsurface storm flow. In an analysis of both trench flow and upslope piezometric measurements for a hillslope site at the University of British Columbia's

Research Forest, *Hutchinson and Moore* [2000] found subsurface flowlines shifted from a control by the confining basal till layer at low flows to a control by the surface topography at high flows. They also found, similar to *Tsuboyama et al.* [1994], that macropore features could be more important than these topographic controls, especially at smaller spatial scales.

[6] At larger scales, *Genereux et al.* [1993] report that the variability in lateral subsurface flow contributions to streamflow, identified using dilution gauging in the West fork of the Walker Branch catchment, were primarily controlled by structures in the dolomitic bedrock geology. Similarly in a glacial till environment, *Hinton et al.* [1993] determined that a combination of topography, sediment thickness and hydraulic conductivity were required to understand the dynamics of groundwater flow and stream discharge.

[7] Our research adds to this body of literature by examining the following questions. What are the first order topographic controls on lateral subsurface storm flow? Can a linkage be made between the dynamics of subsurface storm flow at the trench face with changing upslope soil moisture conditions? During rainstorms how much variability is there in both runoff contributions along the trench face and soil moisture conditions upslope? Observations of hillslope discharge from multiple sections of a trench dug to granite bedrock are here combined with detailed tensiometric data in the area contributing to the trench. Both trench outflows and the patterns of soil moisture status are compared to patterns of the upslope contributing areas and topographic index derived using both soil surface and bedrock surface topography.

2. Study Site

[8] The 41 ha Panola Mountain Research Watershed (PMRW) is situated in the Georgia Piedmont, 25 km SE of Atlanta (Figure 1a) in the Panola State Conservation Park, Stockbridge, Georgia ($84°10'W$, $33°37'N$). Elevation ranges from 222 to 279 m above sea level. Soils are broadly sandy loams, Inceptisols of the Ashlar series and Ultisols of the Gwinnett and Pacolet series, varying in depth from 60 to 100 cm, colluvial on hillslopes and alluvial in the valley bottom. They are highly weathered, especially on hillslopes and ridgetops [Shanley, 1989]. The regolith is highly variable in depth, ranging from less than 1 m on the hillslopes (which can include areas of rock outcrops) to 5–10 m in the valley bottoms. The bedrock is dominated by Panola Granite (granodiorite composition) at higher elevations of the watershed and pods and lenses of the Clairmont formation, a granitic gneiss which is locally amphibolitic, at lower elevations [Atkins and Higgins, 1980]. The watershed is 93% forested with approximately equal percentages of deciduous, coniferous and mixed forest [Carter, 1978].

[9] Research at PMRW was initiated by the U.S. Geological Survey in 1984 as part of the National Acid Precipitation Assessment Program. To date, most of the research has focused on understanding the geochemical input/output budgets and cycling throughout the watershed [Huntington et al., 1993]. Recent intensive studies in the upper 10 ha southeastern branch of the watershed (Figure 1a) have gained insight into the hydrological response of the hillslopes [Freer et al., 1997], hillslope geochemistry [Burns et al., 1998], preferential flow [Peters and Ratcliffe, 1998; McIntosh et al., 1999] and the saturated valley bottom zone and its linkages to the hillslopes [Ratcliffe et al., 1996; Peters and Ratcliffe, 1998].

[10] Annual rainfall averages 1279 mm (range 760–1580 mm) from 1985 to present. Rainfalls are typically convective high intensity short duration in summer and frontal lower intensity and longer duration in winter [Shanley and Peters, 1993]. Analysis of hydrological data from PMRW shows significant seasonal variation in runoff, and evapotranspiration within the catchment. The stream at the 41 ha lower gauge is perennial but once leaf-out has occurred in early April streamflow at the 10 ha gauge site becomes intermittent, flowing only after moderate to large rainstorms. Within the 10 ha subcatchment Peters and Ratcliffe [1998] showed that the 3 ha bare granite outcrop exposed on its North facing slope is a major source of peak storm runoff. The trenched hillslope is situated in this 10 ha upper watershed (Figures 1a and 1b). This subcatchment is completely underlain by Panola Granite and the soils for this upper watershed are typically Ultisols.

3. Hillslope Field Methods and Equipment Installation

[11] The trench study area is located 30 m from the stream channel on a SE facing deciduous forest slope. The study hillslope was characteristic of much of the soil mantled portions of the 10 ha subcatchment. Slope gradients average $25°$, comparable with the mean side slope angles within the 10 ha subcatchment. Hillslope topography across the slope is planar except for a small surface depression near the center of the plot that is more apparent in the upper section of the slope.

The topographic features of the trench hillslope are similar to those of the entire SE facing hillslope at PMRW. The study area is 20×48 m (upslope), with the upper hillslope bounded by a small granite outcrop across the width of the slope that extends to the crest of the slope (<5 m). The trench location was selected based on further practical reasons: access to the site by digging machine, proximity to the slope base but positioned upslope of the riparian zone break-in-slope. While a few other potential slope sections meeting these criteria were considered for study, the upslope outcrop boundary was thought to provide a better condition to define an area (and volume) for water balance computation.

3.1. Trench Site and Subsurface Flow Collection

[12] A 20 m long by 1.5 m wide artificial trench was excavated to bedrock along the lower boundary of the hillslope site. The considerable length of the excavated trench ensured that any changes to flowlines at the trench margins would not affect most trench sections [Atkinson, 1978]. This area was then covered by a roofing structure and sidewalls to prevent direct rainfall inputs into the trench area. Depths to the bedrock surface along the trench face were highly variable (0.05–1.32 m, average = 0.84 m, see profile in Figure 1c). Following the approach of Woods and Rowe [1996], subsurface trench flow was collected for 10 separate 2 m sections for the whole soil profile by partitioning the flow along the bedrock surface using plastic walls (10 cm high) sealed to the rock surface with epoxy. Each section was drained to a separate tipping bucket using a network (<10 m in length) of pipes. During an early January 1996 storm, while work on the trench structure was still in progress, observed contributions of subsurface flow from four obvious macropores (Figure 1c) suggested that these flows should be collected separately.
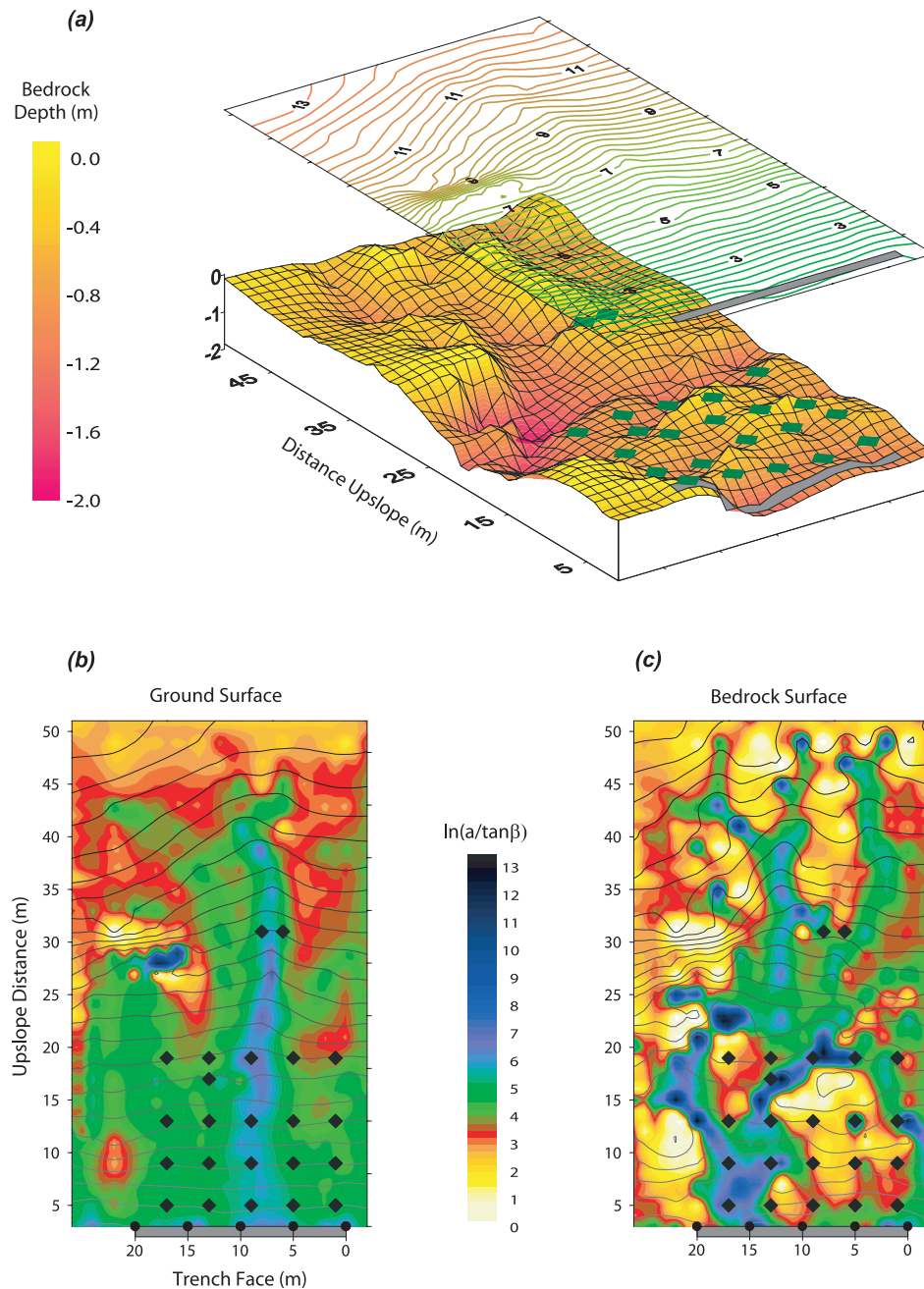
[13] The tipping buckets were leveled and fixed to a solid structure to prevent "chattering" between buckets. All flow was routed from the tipping bucket gauge house downslope to drain into the 30 m slope area before the stream. Two bucket capacities were used (125 and 250 mL per tip), the larger buckets were connected to the largest flowing macropores. Accumulated bucket tips were recorded every 15 s using two pulse channel multiplexers connected to a Campbell CR10 data logger. Calibration of the tipping buckets before installation showed that a dynamic loss needed to be accounted for as the number of tips per minute increased due to spillage. The buckets were rated up to their maximum working tip rate of 60–70 tips per minute (~8.5 and 17.5 L/min for small and large buckets, respectively).

[14] To assess a total flow for each trench section, flow from the macropores was apportioned between two neighboring trench sections dependent on distance between the two section centers as;

$$P_a = L_a^{-1}/\left(L_a^{-1} + L_b^{-1}\right) \quad \text{and} \quad P_b = 1 - P_a \qquad (1)$$

where L_a and L_b are the distances between the two nearest trench section centers (a and b) and P_a and P_b are their respective contribution proportions. The rational for this proportional sharing is to take into account the difficulty of defining strict boundaries between sections upslope of the trench. This proportional sharing is an attempt to allow for the possible contributing areas of the macropore flow

Figure 2. Hillslope DTA results: (a) depth to bedrock survey results, (b) topographic indices for both ground surface, and (c) bedrock topography. The green (Figure 2a) and black (Figures 2b and 2c) diamonds show the colocated tensiometer positions throughout the slope.

seen at the trench face [*Tsukamoto and Ohta*, 1988; *McDonnell*, 1990].

3.2. Hillslope and Tensiometer Installation

[15] The hillslope was surveyed on a 2 m grid that extended across the slope beyond the 20 m width of the trench using a laser sighted total station (288 points in total). Depth to bedrock measurements were taken on the same survey grid network using either a 2.54 cm soil corer forced down to refusal, or if the depth became greater than 1.25 m, a small hand auger was used to complete the measurement.

Depth to bedrock was highly variable (0–1.83 m, mean 0.63 m) throughout the slope (Figure 2a). Mapped mean soil depth was within a few centimeters of the catchment average soil depth (0.6 m) mapped on a coarser grid [*Zumbuhl*, 1998]. Once this survey was completed all the holes were filled with 2.54 cm plastic access tubes, slotted for the bottom 20 cm to enable the collection of saturated subsurface flow for chemistry samples (details given by *Burns et al.* [1998]).

[16] To understand the spatial dynamics of the hillslope response a grid of recording colocated tensiometers were

installed (shallow/deep pairs) primarily in the lower half of the hillslope site (Figure 1b). The tensiometers used Honeywell wet port pressure transducers (±15 psi) with Soil Moisture Corporation 1 bar high flow ceramic cups. Tensiometer response times showed no lag when compared to the responses of TDR readings at a nearby hillslope site. The tensiometers were continuously recorded throughout the study period using two Campbell 32 channel multiplexers connected to a CR10 data logger. This network gave a total of 42 tensiometers within the study area equally spaced at 2, 6, 10, 16 m upslope (one set at 14 m) and 1, 5, 9, 13, 17 m across the slope from the right-hand side of the trench face. The average depth of the shallow tensiometers was 20 cm and of the deep tensiometers was 62 cm. Field calibration of colocated tensiometer pairs throughout the hillslope suggested that the general relationship between negative capillary potential and height above a known water table was effectively linear, similar to that observed by *Burt and Butcher* [1985]. The matrix potential readings for the deep tensiometers were used to estimate the water table level. For the storm periods reported here, where the spatial pattern of saturation is of interest, the deep tensiometers were close to or below the water table level. Therefore the estimates of the water table level are assumed to be relatively accurate.

[17] Hydrometric data were collected concurrently at the main PMRW meteorological station downstream from the 41 ha lower gauge. Losses relating to interception storage were ignored for the period of this study as leaf out had not yet occurred.

3.3. Digital Terrain Analyses (DTA)

[18] Both the accumulated upslope contributing area and the topographic index of *Kirkby* [1975] were calculated using the multiple direction flow algorithm of *Quinn et al.* [1991] from a 1 m DTM interpolated from the surveyed grid of data described above. The index is defined as $\ln(a/\tan \beta)$, where a is the upslope accumulated area and $\tan \beta$ is the local slope angle. We changed the normal algorithm calculations in this study only for cells identified as being adjacent to the trench face. Such cells did not share accumulated area downslope to neighboring cells that were adjacent to the trench face. This was thought to be inappropriate due to the nature of the flow collection that was constructed at the trench face (changes to index values were negligible). Two sets of accumulated upslope area and topographic indices were calculated, one using the ground surface topography for the slope ($SURF_{acc}$ and $SURF_{atb}$) and one the surface of the soil–bedrock interface (BR_{acc} and BR_{atb},) called the bedrock surface (i.e., the assumed impeding layer). Figures 2b and 2c show the results of these two analyses (for the $SURF_{atb}$ and BR_{atb} indices) which clearly show that by taking into account the underlying bedrock topography the areas of flow convergence (equating to higher values of the indices) have been altered significantly throughout the hillslope.

[19] Across the trench face the highest BR_{atb} values occur where the soil depths are greatest (12–16 m from the right of the trench face, see also Figure 3a). This observation would perhaps be expected as this is indicative of greater soil depths that extend upslope from this area (Figure 2a). For this slope, accounting for the depth to bedrock spatially has a significant effect on the pattern of accumulated area convergence that primarily controls the spatial variations in

the index values. These DTA results can now form the basis for a study of which spatial pattern of flow convergence best describes the dynamics of subsurface storm flow at the trench face and the spatial variations in soil moisture throughout the slope.
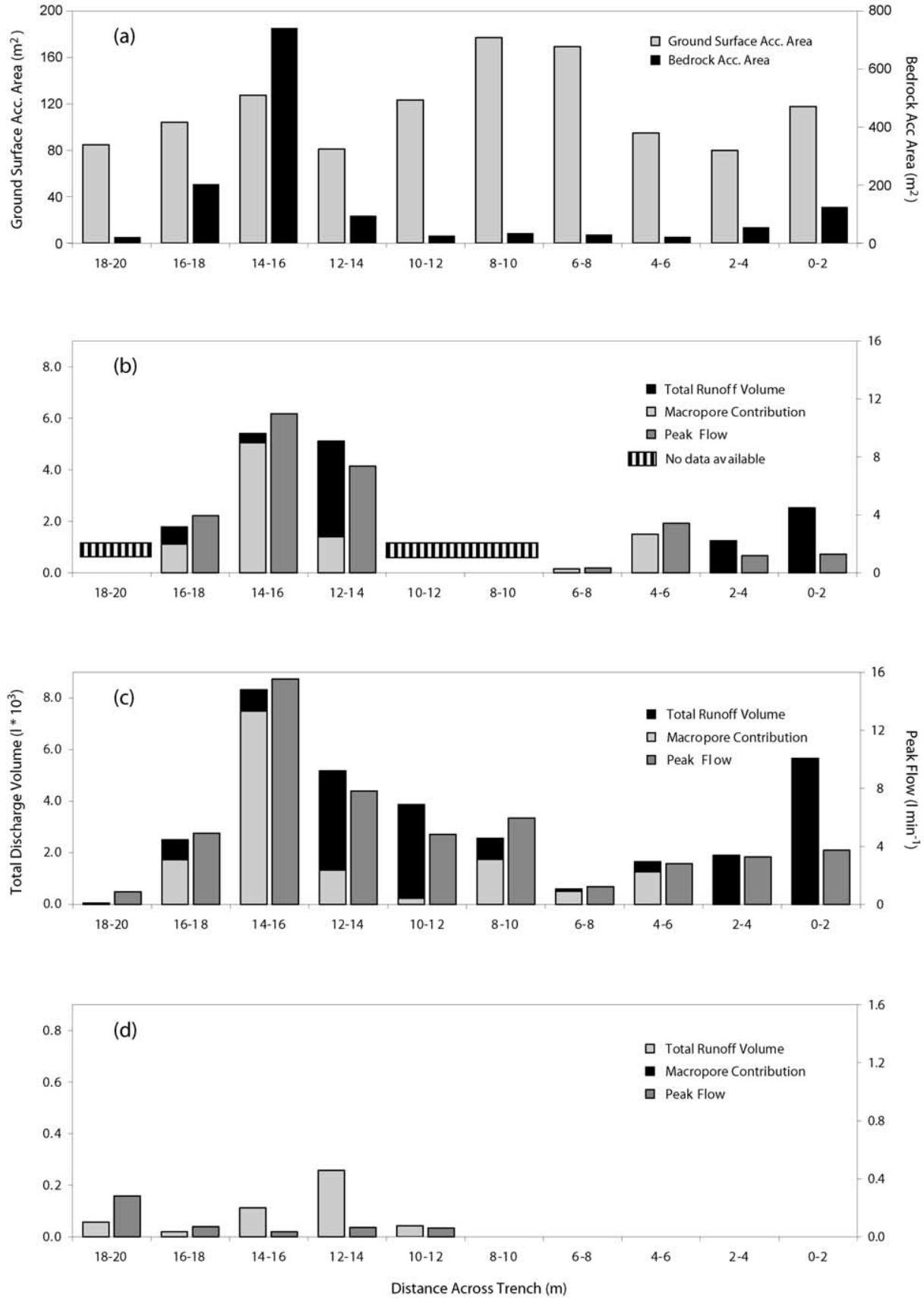
4. Results

4.1. Study Periods

[20] Collection of trench flow began in January 1996 during the hydrologically active season, when the catchment is generally wet and the hillslope connectivity to the valley bottom saturated zone was high. Three main rainstorms occurred (4 February, 6 March, and 27 March) during the period of study in 1996 (Table 1). The three rainstorms vary in magnitude, antecedent soil moisture status, and amount of runoff produced. This paper explores each rainstorm in terms of cumulative subsurface flow, but only evaluates the largest rainstorm (6 March) in greater detail using trench discharge and spatial water table variations for different ''snapshot'' time sequences. No overland flow was observed during any of the rainstorms near the trench face.

4.2. Timing of Observed Trench Flow Responses

[21] Trench face storm flow responses are complex. Individual sections of the trench have significantly different flow rates, response times (including no flow responses) and recession characteristics. These characteristics are summarized in Tables 2 and 3 (see also Figure 4c which shows the recorded trench outflows for the 6 March rainstorm). The results listed in Table 3 for the 6 March rainstorm typify the relative response characteristics of the trench sections to large rainstorms. Rain from the first part of the storm, totaling 48.5 mm, did not induce significant increases in trench flow due to the relatively dry antecedent conditions (Figure 4d, average prestorm soil moisture tension in the slope was −77 cm H_2O for shallow and −52 cm H_2O for the deep tensiometers). Timings for the trench responses are taken from the start of the second part of the double peaked rainstorm (7 March 1996, 0020).

[22] Times of initial rise (defined as the point when flow reaches 5% of the peak) show a considerable range among trench sections (0152–0648 hours). The right and middle sections of the trench (0–10 m) have a significant lag time before the initiation of matrix flow, although the macropore responses in these sections (Figure 1c, macropores, Figures 1d and 1e) are much quicker ($\overline{T}_{ini}$ = 0452 hours). The matrix flow in the deeper left-hand section (10–16 m) responds approximately twice as fast as the right-hand section. However, both time-to-peak and recession characteristics are similar for most of the trench (4–16 m). The much longer recession characteristics of the far right trench section, which appears to be matrix flow dominated, implies that these features of the flows reflect different subsurface flow regimes upslope. The more rapid responses and lower total volumes of flow on the far left-hand side (16–20 m) are characteristic of the shallow soil depths. Macropore responses have consistently more rapid time to peak and recessions compared to those of the matrix flows in all except the shallowest trench sections. The initial rapid decline in total trench flow is caused mainly by the macropore reces-

Table 1. Summary of the Main Rainstorms Studied in 1996

Data	4 February	6 March	27 March
Total rainfall (mm)	60	95	25
Storm return period (days)	150[a]	975[a]	27[a]
API_7 (mm)	0.87	0.12	0.55
Total trenchflow Q_{tot} (L)	17,500[b]	32,300	490
Trenchflow Q/P (%)	23.5[b]	27.0	1.6
10 ha Q_{max} (L/min)	83.5	121.0	18.1
10 ha Q/P (%)	56	33	14
Total macropore contribution (%)	46.7[b]	45.7	0.0

[a]Return period based on 16 years of rainstorm data from PMRW.
[b]Different to true observed due to some trench sections not being monitored for this rainstorm.

sions, approximately 0145 hours after the cessation of rainfall (~0555 hours after the peak of the rainstorm).

[23] If the time-to-peak and recession characteristics of the trench flow responses are used to characterize the general flow regime upslope, then the trench can be classified as having three distinct flow responses. The middle and deeper sections of the trench (4–16 m) characterize the majority of the trench sections; the macropore and shallow left trench sections (16–20 m) give much more rapid times to peak and recession responses, suggestive of more rapid and/or preferential flow processes; and the right side of the trench (0–4 m) has much slower responses (times to peak, 50% and 20% recession are 177%, 153% and 151% longer respectively), indicative of soil matrix dominated flow.

4.3. Overall Cumulative Subsurface Storm Flow

[24] Figures 3b–3d show both the total cumulative flow and peak subsurface flow for each trench section for the three rainstorms. Contributions from individual trench sections are separated into macropore and matrix flow responses for sections where significant macropore flow features were individually monitored.

[25] Results from the largest two rainstorms (4 February and 6 March) indicate that deeper trench sections dominated total subsurface storm flow and peak flow responses. Macropore contributions were 45% of total storm flow for the 6 March rainstorm, of which 32% can be attributed to the two macropores located in the deepest trench face section (14–16 m). Macropore contributions to total storm flow were 46% for the 4 February rainstorm (although this figure is affected by some missing data for trench sections without completed tipping bucket installations). What is interesting about these two rainstorms is the similarity of total flow accumulated for section 12–14 m. This trench section was dominated by matrix flow (i.e., no macropore flow occurred). The matrix flow contrasts significantly with the much reduced total flow accumulation for the macropore dominated section 14–16 m for the 4 February rainstorm (65% of 6 March total flow, Figures 3b and 3c). In all cases macropore flow receded very rapidly after the end of the rainstorm.

[26] In contrast, the 27 March rainstorm was small (25 mm), with drier antecedent conditions, producing very little

response at the trench face and no macropore flow as seen in Figure 3d (note the 10^{-1} reduced axis scales).

4.4. Relationships Between Cumulative Trench Flow and the $SURF_{acc}$ and BR_{acc} Indices

[27] Figure 3a shows the patterns of the two upslope-accumulated areas along the trench face. Values are averaged over the 2 m trench section from the 1 m DTA analysis. Figure 3a shows that the pattern of the $SURF_{acc}$ is relatively constant across the trench face (range = 79–167 m^2, note different scaled axes). Peak values near the center of the slope (6–10 m) are the result of upslope area accumulations from a small hollow which is only clearly defined 20 m upslope from the trench face (see Figure 2b). Alternatively the BR_{acc} shows a much more varied pattern across the slope (range 21–735 m^2), with the larger peak value associated with the deepest trench section (14–16 m).

[28] Results relating the upslope accumulated area to the total trench flow for the 6 March rainstorm clearly indicate that the patterns of the BR_{acc} are much better correlated with both the trench flow data than the $SURF_{acc}$. This is further indicated in the R^2 statistics where the ground surface index shows no correlation with the trench flow characteristics (flow volume: $R^2 = 0.58$ for BR_{acc} and $R^2 = 0.01$ for $SURF_{acc}$; peak flow: $R^2 = 0.79$ and $R^2 = 0.01$, respectively). Flow pathways therefore seem to be strongly reflecting the bedrock topography control (Figure 2c) on the trench face upslope accumulated areas.

[29] Analysis of the other rainstorms, 4 February and 27 March, suggest that the relationships between the upslope accumulated area and the subsurface storm flow are variable. The first rainstorm, (4 February) was small, but was associated with a much wetter antecedent soil moisture status (Table 1). Although not all trench sections were being monitored during this rainstorm (installation of all trench sections had not yet been completed), the patterns of total subsurface flow are very similar to the larger 6 March rainstorm and produced similar but less significant relationships with the upslope accumulated areas ($R^2 = 0.51$ for BR_{acc} and 0.10 for $SURF_{acc}$ for total subsurface flow). Macropore flow contributes a lot to the total flow (47%), and the runoff coefficient for the slope is similar to that of the 6 March rainstorm.

[30] As expected there was no significant relationship between the upslope accumulated area and the patterns of flow for the very small 27 March rainstorm (both $R^2 < 0.1$), with only five sections of the trench producing a measurable response (10–20 m). Tensiometer observations across the hillslope suggest that there was no significant water table development for this rainstorm.

4.5. 6 March Snapshot Subsurface Flow Analyses and Relationships With the Indices

[31] If the suggestion that account must be taken of the dynamic saturated connectivity of the slope to improve index predictions is reasonable, then predictions of trench

Figure 3. (opposite) PMRW trench face, comparison of DTA results with observed cumulative flow and peak flow for the three rainstorms: (a) upslope accumulated areas for the ground surface and bedrock surface, observed volume, and peak flow for (b) 4 February rainstorm, (c) 6 March rainstorm, and (d) 27 March rainstorm (note that scale is reduced 10 times for both total flow and peak flow for this rainstorm).

Table 2. Trench Face Characteristics, Observations of the Individual Trench Sections

Trench Section Type	Description of Flow Responses
0−2 and 2−4 m	Deeper right-hand section. Matrix-dominated flow, long recession duration, long rainfall response time and time to peak
4−6, 6−8, and 8−10 m	Shallow middle section. Only produces flow after large rainstorms, hence long response times (macropore dominates volume in 4−6 m).
10−12, 12−14, and 14−16 m	Main deep section. 12−16 m seep at low flow conditions and are the deepest trench sections, 10−12 m is between this and above. Quicker response but similar recessions to previous section. Macropore flow dominates 14−16 m.
16−18 and 18−20 m	Shallow left section, responds quickly to rainstorms but has short-lived recessions. 16−18 m has a small deep section with significant macropore flow.
All macropores	Slower to respond than deep matrix flow trench sections, rapid times to peak and rapid recession characteristics.

flow patterns should improve during moderate to large rainstorms (using the basic index assumptions) when the slope becomes more hydrologically connected. Conversely, these predictions should be worse during wetting up periods and during later recession periods, when saturated conditions dissipate. Furthermore, results from such periods should be better than those obtained for the overall cumulative storm flow predictions, as much of the total flow accumulations occur during drier periods. The cumulative flow for a rainstorm also disguises the variability along the trench face temporally because flows are switching (in relevant sections) between matrix flow dominated waters to macropore dominated and back again. This clearly affects the proportional contributions of flow from each section to overall trench flow, which is further altered by the timings and characteristics of individual matrix flow responses.

[32] To assess whether predictions improve during the wetter periods of the rainstorm, a temporal sequence of "snapshots" of subsurface trench flows was evaluated. Figure 4 shows the time of each snapshot (a–o). Figure 5 shows some of these snapshot periods for spatial patterns of subsurface flow along the trench face and water table heights above the bedrock surface throughout the slope (the water table results will be presented below). The trench and hillslope conditions for each snapshot periods are summarized in Table 4.

[33] Similar to the results presented by *Woods and Rowe* [1996], the relative proportions of flow among trench sections are not temporally constant (Figure 5, see also Figure 4a). Peak trench flow (Figure 5f, ~41 L/min) occurs at 0640 on the 7 March prior to flow initialization in the 0−2 m trench section. The importance of the 0−2 m section delayed contribution to subsurface flow can be

seen clearly during the recession period (Figures 4a and 5j−5o). This contribution becomes dominant near the end of the trench storm response.

[34] The $SURF_{acc}$ index does not predict any of the patterns of subsurface flow during these snapshot periods ($R^2 = 0.02$). However, the relationships between the flow patterns and the BR_{acc} index appear better correlated for the wetter periods of the 6 March rainstorm (Figures 5e−5j), with $R^2 = 0.80$ for snapshot g, see Table 4), as shown by the spatial distribution of the development of the water table (Figures 5e−5j). It is noted that these correlations are much better than those obtained for the total cumulative trench flow for this rainstorm. Furthermore the predictions of flow patterns using the BR_{acc} index, as described by the R^2 relationship, rapidly decrease during the recession period and prior to water table development occurring throughout the slope (see next section, Figure 6).

[35] Although the BR_{acc} index does not have the highest correlation with the trench flow at the peak (see Figure 6), the period of high correlation coincides with the greatest water table development spatially, as described by the tensiometer responses (see below). Given that macropore contributions dominate peak trench flow (72%), it is feasible that the soil matrix moisture conditions will not capture the characteristics of these rapid preferential flow responses, but will best describe the overall hydrological connectivity of the slope.

4.6. Observed Spatial Water Table Responses and Linkages to the Topographic Indices

[36] The spatial patterns of water table development above the bedrock surface are presented in Figure 5 for the same snapshot periods as those previously discussed for the trench flow data. Each of these periods is further
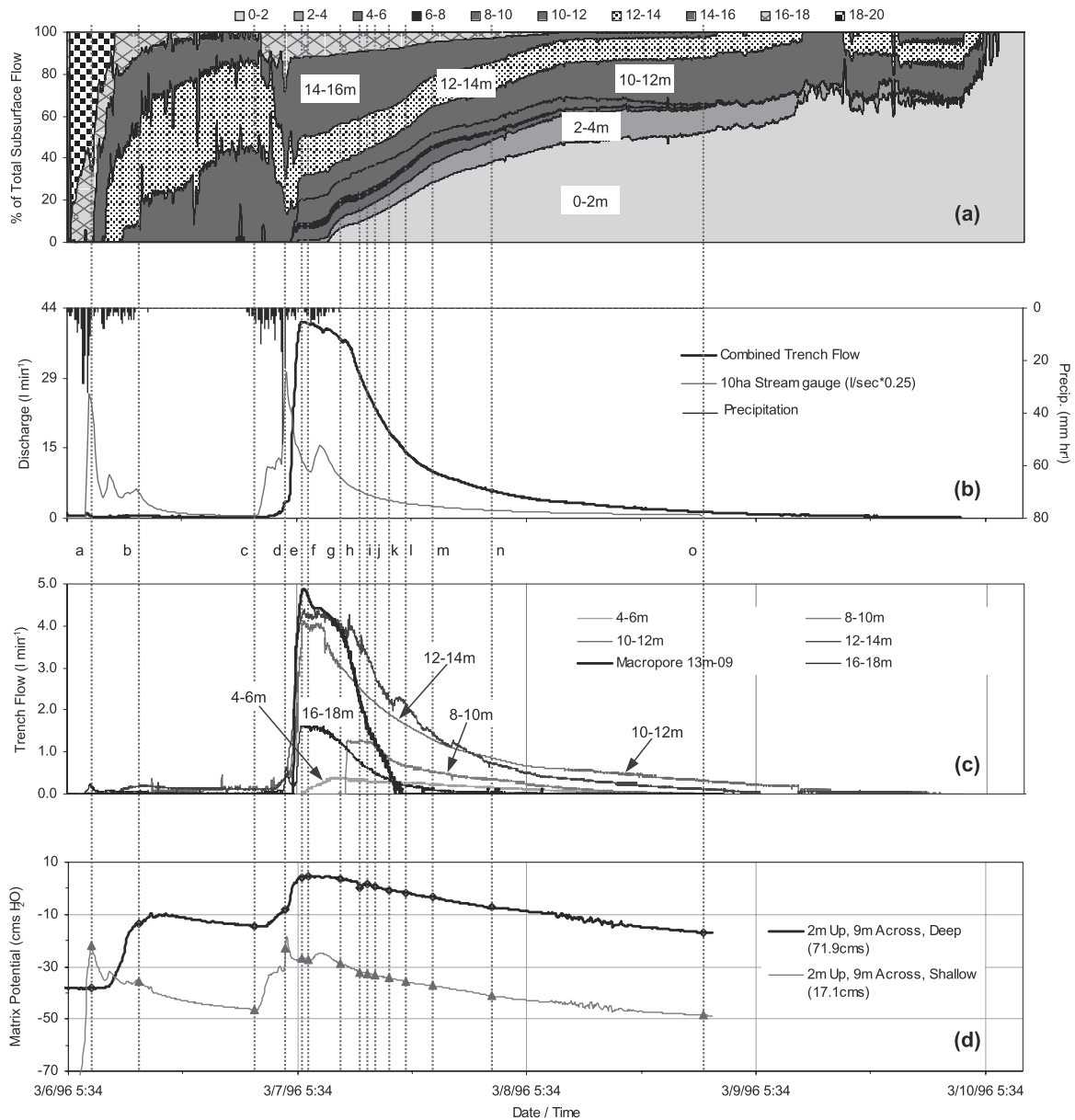
Table 3. Trench Face Characteristics, Numerical Observations from the 6 March Rainstorm

Trench Section	Timing of Trench Responses,[a] hours				Total Trench Flow for Each Section, %	Macropore Flow for Trench Section, %
	T_{ini}	T_{peak}	$T_{50\%}$	$T_{20\%}$		
0−2 and 2−4 m	0648	0550	1246	2940	23.3	23.4
4−6, 6−8, and 8−10 m	0634	0303	0815	1958	3.0	14.9
10−12, 12−14, and 14−16 m	0242	0316	0813	1942	25.5	53.8
16−18 and 18−20 m	0152	0233	0536[b]	0910[b]	2.5	7.9
All macropores	0448	0203	0509	0827	45.7	n/a

[a]T_{ini}, T_{peak}, $T_{50\%}$, and $T_{20\%}$ = Time to initialize, time to peak, and recession time from peak to 50% and 20% of peak flow respectfully (averaged for sections, macropores calculated separately).
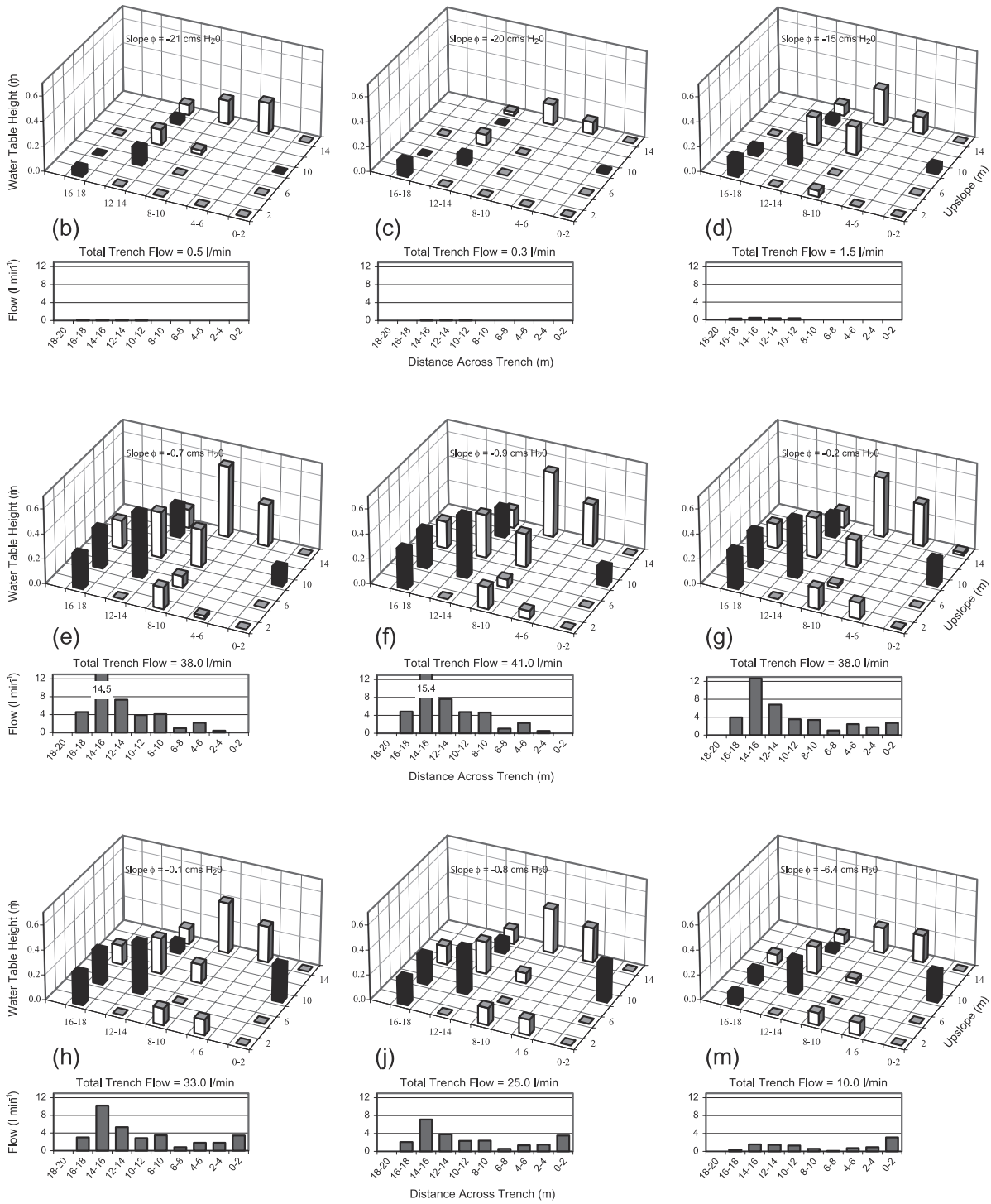[b]Only included data from 16 to 18 m.

Figure 4.   The dynamics of discharge and matrix potentials for the 6 March rainstorm: (a) proportions of subsurface discharge, (b) total trench flow and subcatchment stream discharge, (c) a selection of trench section responses and a macropore response, and (d) a colocated shallow and deep tensiometer response for one hillslope position.

characterized by the average matrix potentials, adjusted to the 62 cm average depth, for all deep tensiometers (Figure 5). We wish to add at this point a cautionary note concerning methodologies that attempt to interpolate point soil moisture data over complex subsurface terrain. Such interpolations could be inappropriate when the length scale of variation in the bedrock topography is much less than the distance between the soil moisture measurement points if the interpolation methods used do not take into account any intervening local divides.

[37]   The general characteristics of the colocated tensiometer readings are shown in Figure 4d. The shallow tensiometers respond more rapidly and have more transient peaks than the deep tensiometers (suggestive of wetting

front propagation from rainfall inputs). For this colocated site shown in Figure 4d (02–09), the response of the deep tensiometer to the second rainstorm corresponds with the increases in flows observed at the trench face. However, significant variations in tensiometer responses occur throughout the slope (see below).

[38]   Average prestorm conditions for the lower slope for each upslope grid row, suggest a positive gradation of soil moisture conditions downslope (from −65 to −41 cm H$_2$O). However, the development of a simple saturated wedge, expanding upslope during the rainstorm, is not evident. Such development appears to be occurring and expanding from the bedrock hollows throughout the slope (similar to the work of *Tsuboyama et al.* [1994]).

Figure 5. Trench subsurface flow and water table observations for a selection of the snapshot periods denoted by letter and detailed in Table 3. The two-dimensional column graph shows trench flow for individual sections, where % is macropore discharge in total flow, and the three-dimensional column graph shows the water table height. Black columns denote grid cells in areas of higher topographic convergence as defined be the bedrock topographic surface.

Therefore the spatial development of saturation appears to be directly related to the zones of high upslope accumulated area (as denoted by high values of the BR_{atb} index, see Figure 2b). These areas of saturation progressively expand downslope during the rainstorm (Figures 5c–5f). The spatial development of water tables is complex and the relative saturated development throughout the slope is not constant over time. The matrix potentials of most of the deep tensiometers are positive at peak flows.

Table 4. Details of Time Periods Used in the Discharge and Spatial Analyses for the 6 March Rainstorm

| | Correlations (R^2) With Bedrock Index | | Slope Condition | | | |
| | Trench Discharge | Water Table | Soil Moisture Conditions (cm H_2O)[a] | | | |
Id Date/Time (% Rainfall Total)			ϕ_s	ϕ_l	ϕ_r	Comments on Slope Response
(a) 6 March 1996, 0800 (33)	0.02	0.14	−21.5	−23.6	−37.7	First peak of shallow tensiometer responses
(b) 6 March 1996, 1300 (48)	0.18	0.33	−21.0	−25.3	−31.8	First peak of deep tensiometer responses
(c) 7 March 1996, 0100 (51)	0.01	0.53	−15.4	−20.5	−29.9	At start of shallow tensiometer response
(d) 7 March 1996, 0420 (82)	0.42	0.46	−0.6	−10.5	−20.1	Second peak of shallow tensiometers
(e) 7 March 1996, 0600 (86)	0.73	0.48	−1.1	−10.8	−19.1	Peak water table development in central area of the slope
(f) 7 March 1996, 0641 (87)	0.72	0.52	−0.1	−12.2	−13.3	Near peak of deep tensiometers
(g) 7 March 1996, 1000 (95)	0.80	0.63	−2.2	−14.2	−13.8	Peak of deep tensiometers and water table development in right section of the hillslope
(h) 7 March 1996, 1200 (end)	0.79	0.68	−3.2	−14.8	−14.3	Central hillslope area is reducing matrix potentials more rapidly
(i) 7 March 1996, 1252	0.76	0.64	−3.7	−15.1	−14.8	As previous
(j) 7 March 1996, 1341	0.73	0.62	−5.2	−15.9	−16.2	As previous
(k) 7 March 1996, 1511	0.64	0.55	−7.3	−17.3	−17.7	Beginning of main matrix potential recessions throughout the slope
(l) 7 March 1996, 1654	0.35	0.54	−9.8	−18.5	−20.6	
(m) 7 March 1996, 1938	0.08	0.45	−15.9	−22.5	−26.0	
(n) 8 March 1996, 0153	0.00	0.37	−26.6	−28.7	−36.7	
(o) 9 March 1996, 0000	0.01	0.17	−21.5	−23.6	−37.7	

[a]Here ϕ_s, ϕ_l, and ϕ_r are average soil moisture conditions for all, left, and right slope areas, respectively.
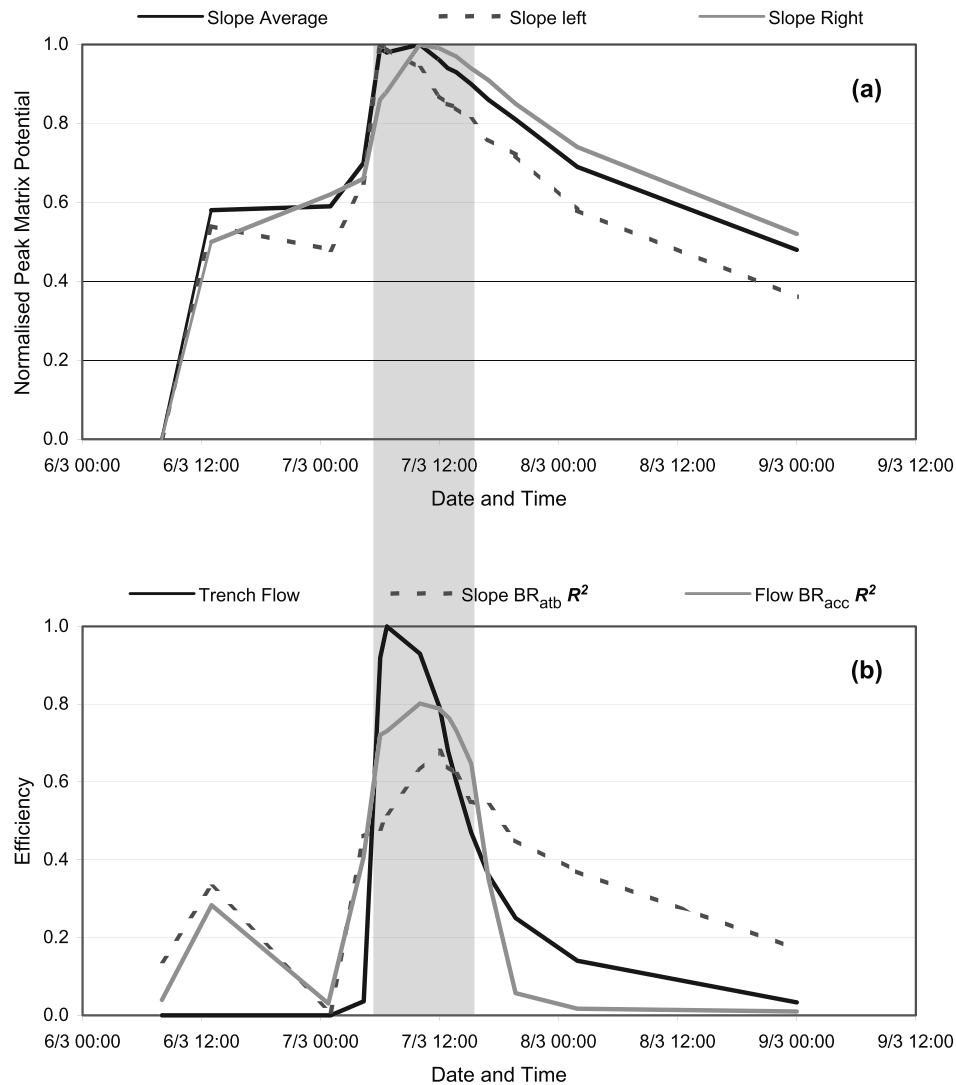
[39] Spatial variation in the timing of the slope response is linked with the trench face flows, especially with regard to the initialization of trench flow and time to peak. The tensiometers associated with flow accumulation (as described by the BR_{atb} index) for the deep left section of the trench (e.g., tensiometers > 9 m across the slope, plus tensiometer 16 m up, 5 m across, see Figure 2c) respond differently to those for the far right section. For the second peak, the average time to peak from the initial response was 0318 hours for the left section and the average peak response was at 0542 on 7 March, some 45 min prior to the peak trench flow response. The average time to peak was 0815 hours for the right section and the average peak response was at 1200 on 7 March, which is closely related to the delayed peak response of the 0−2 m section of the trench. This delayed peak response for the deep tensiometers situated within the right section of the hillslope is the reason why the greatest mean slope matrix potentials occur during the trench flow recession period, when this area becomes more hydrologically connected upslope (Figures 5g−5j).

[40] Recession characteristics for these groups of tensiometers do not show any clear differences in their form (time to 50% of peak response $R_{50\%}$ = 1218 and 1252 hours; time to 20% of peak response $R_{20\%}$ = 2046 and 2120 hours for left and right sections, respectively). However, a 6−7 hours delay occurs before the recession, which is similar to that for the peak flow response. The tensiometer responses were expected to have some relationship to the trench flow responses. The differences observed in flow responses for sections of the trench can be seen throughout the slope in the water table responses (given the limitations of the spatial coverage) if tensiometers are grouped according to the flowpaths identified by the BR_{atb} index.

[41] Predictions of the water table responses using the two topographic indices were made for each temporal snapshot period by comparing the values of the indices with the depth to the water table. Table 4 lists the R^2 fits of these relationships for the BR_{atb} index, fits for the $SURF_{atb}$ index produced no significant correlations with the spatial water table responses (maximum R^2 = 0.05). Similar to the results presented for the trench flows, the relationships between the BR_{atb} index and the depths to the water table are better correlated for the wetter hillslope conditions. The linkages between the wettest slope conditions, and the best correlations of the BR_{acc} and BR_{atb} indices to trench flow and water table development, respectively, are clearly identified using the temporal snapshots (see Figure 6).

5. Discussion

[42] Our results show the importance of the bedrock surface, representing the effective hydrological impeding layer, in controlling the spatial dynamics of hillslope wetting, water table development and generation of lateral subsurface storm flow. Results from three rainstorms of varying magnitude show that the patterns of trench face flows and water table development are generally much more related to the drainage area associated with the bedrock surface than the drainage area associated with the ground surface. However, this relationship is not apparent for any of the topographic indices for the smallest rainstorm, where the observations suggest that the hydraulic connectivity of the slope is not so well developed. The importance of slope connectivity on the prediction of trench flow and water table dynamics has been further emphasized by analyzing a sequence of temporal snapshots for the 6 March storm. These results show a

Figure 6. Temporal relationship between (a) slope soil moisture conditions and (b) trench discharge (normalized to peak flow) and R^2 relationships of BR_{acc} (for trench flow) and BR_{atb} (for water table height) for the 6 March rainstorm (note that shaded area denotes $R^2 > 0.6$ for trench flow relationship with BR_{acc}).

significant increase in the predictive capabilities of the bedrock-derived indices occurs during peak soil moisture wetness conditions. This result would be expected since the use of a topographically derived index assumes continuity of lateral subsurface flow to the divide and is an indication that, in environments such as PMRW, a more dynamic representation of the flow dynamics and continuity of flow pathways will be necessary [*Barling et al.*, 1994; *Freer et al.*, 1997; *Beven and Freer*, 2001]. In what follows we discuss in more detail the mechanism of bedrock control on subsurface storm flow, concentrating on the hillslope storm flow responses; the potential for model development; and the importance of these results at the catchment scale.

5.1. Bedrock-Controlled Flow Pathway System

[43] As well as the soil development and catenary sequences observed by *McIntosh et al.* [1999] in this catchment, soil depths catchment-wide have been affected

by human-induced erosion in the last century, due to intensive cotton cultivation on these submarginal lands. These accelerated erosion rates can be seen in gully-like features around the catchment. However, none of these gullies appear to be eroded down to the soil–bedrock or soil–saprolite interface. Thus, these historical erosion processes do not appear responsible for any of the bedrock topography mapped at our site or other sites in the vicinity.

[44] Much of the internal tensiometer response suggests that some water bypasses the bulk soil matrix (as described by *McIntosh et al.* [1999] at the site) and perches at the soil–bedrock interface. Filling of storage in this lower soil profile provides a threshold constraint for the development of a water table and lateral downslope flow in connected saturated zones. It appears that much of this rapidly responding downslope flow is stored or "old" water displaced from the soil during a rainstorm [*Burns et al.*, 1998]. The conceptual model is that, above a certain threshold of wetting, only a very small amount of bypass

flow to depth is required to fill storage in the deepest soil layers and drive saturated lateral preferential flow at the soil–bedrock interface. This mechanism has similarities to that described by *Tsuboyama et al.* [1994], where a preferential flow system (primarily evolved within bedrock channels and depressions) interacts rapidly with the surrounding mesopore structures, which act as connecting nodes within the hillslope continuum. The macropore contributions for trench section 14–16 m appear to be the result of a longer flowpath length within the slope, requiring a higher storage threshold to be satisfied before connectivity of the pipe network is achieved (in this case due to the much greater rainfall totals for the 6 March rainstorm). These controls also determine the base cation concentration and flushing at the hillslope scale, as described by *Burns et al.* [1998]. Our results have also shown that variations in the responses of soil moisture responses within upslope flowpaths are linked to the variations of trench flow responses. This has clearly been shown by the different storm flow dynamics of trench section 0–2 m, where delayed hillslope matrix potentials and trench flow responses are suggestive that this more matrix flow dominated system, can be an important, albeit a significantly delayed, contribution to trench flow.

5.2. Macropore Contributions

[45] The macropore flow data in this paper warrant further study. We have no data to quantify connectedness upslope and indeed these may be simply trench face manifestations of transient groundwater seepage. Notwithstanding these deficiencies, *Burns et al.* [1998] did show that flow from our monitored soil pipes was dilute in base cation concentration relative to matrix seepage from elsewhere across the trench face. This would suggest that pipes at the trench face might integrate a connected flow system that extends several meters upslope along the bedrock flowpath. This connection may include various micro–meso–macropore connections along the narrow ribbon of mobile flow as inferred from the patterns of Figure 2.

[46] While our findings are not new in terms of recognizing significant contributions of macropore to subsurface flow [*Gilman and Newson*, 1980], the qualitative relation between preferential pathways and the bedrock topographic index is new and possibly important. *Jones* [1997] commented in his analysis of pipeflow for many rainstorms that shallow ephemeral pipe networks are "particularly efficient rainfall collectors and transmitters," although water in some of these larger ephemeral pipes may also be "old" water [*Sklash et al.*, 1996].

[47] There are several differences between the study site (and results) of *Hutchinson and Moore* [2000] and PMRW, although each study hillslope is underlain by relatively impervious granitic bedrock. One important difference is that macropore flow in the Hutchinson and Moore study became increasingly important with increasing rainstorm magnitude in trench sections that were not dominated by matrix flow. It is possible that the macropores of *Hutchinson and Moore* [2000] connected to upslope saturation controlled by the till surface, but the plot-scale patterns of the till boundary and upslope contributing areas were not available in their paper. As stated previously, the monitored

trench macropores at PMRW were associated with the deepest soils/lowest bedrock surface elevations.

5.3. Modeling Dynamic Subsurface Saturated Areas With Topographic Indices at the Hillslope Scale

[48] Detailed hillslope studies commonly reveal great complexity and heterogeneity in hillslope responses to rainfall [e.g., *McDonnell*, 1990; *Woods and Rowe*, 1996; *Hutchinson and Moore*, 2000]. Furthermore, the initiation of various flow mechanisms may require certain thresholds to be exceeded. Given this complexity it may be somewhat surprising that the flow and water table predictions using the BR_{acc} and BR_{atb} indices in this study have achieved such highly significant results. It is clear, however, that the extent of saturation at the soil–bedrock interface is a dynamic process, and that a simple static index may not be adequate to reflect the changing connectivity of the downslope pathways during the wetting and drying of the hillslopes.

[49] It is also clear that it is not possible to define the nature of the bedrock surface everywhere for hydrological modeling purposes. Nor will it always be the case that the surface is well defined as a sharp (relatively) impermeable boundary. It is easy to envisage other situations where the downslope flows of water will be controlled by other local factors such as channeling through fractures in the bedrock [e.g., *Anderson et al.*, 1997], percolines in saprolite or subsoil [*Bunting*, 1961] or piping in the near surface soil [*Gilman and Newson*, 1980]. Clearly the PMRW results do not support the dynamic shift of flowpath connectivity control from bedrock to surface topography during wetter hillslope conditions, as observed by *Hutchinson and Moore* [2000]. Therefore in each case, the local characteristics and dynamic connectivity of the flow pathways may be important in controlling the hillslope-scale responses, but may be essentially unknowable at the catchment scale [*Beven*, 2000]. Alternatively, as more studies are conducted, patterns of processes may emerge that would allow extrapolation of the dominant flow processes for particular types of bedrock and terrain. Perhaps one of the more important conclusions from the current body of information on hillslope flow processes is that caution is required when using internal state data to evaluate the spatial representation of models without some knowledge of the importance of the underlying subsurface features on the local hydrological responses.

[50] The next step is to quantify this dynamic response and the contributions of mobile subsurface flow from hillslope areas to recharge in the valley bottom saturated zone. The impossibility of knowing all the detailed flow pathways at the hillslope or catchment scale suggests that this will require some form of inductive phenomenological representation. At PMRW, *Hooper et al.* [1998] have suggested that these contributions may not be expressed directly in the channel because trench flow responses lag streamflow and the chemical end-members bounding stream water do not include a strong hillslope component. This remains a fruitful area for further study in a variety of geomorphic settings with different ratios of hillslope to riparian mobile flow volume.

[51] However, in this study a significant part of the total hillslope flow was supplied by 4 macropores over a 20 m section, while patterns of saturation were best described by a

BR_{acc} spatial index pattern, that is highly variable locally, and the development of connected saturation appeared to depend on thresholds of wetting, not yet properly characterized, within the bedrock hollow pathways. Indeed, it should be expected that that given the complexity of the subsurface topography, further variations in the localized patterns of the topographic index and patterns of saturation would be expected if higher resolution data were available. Given this complexity of the hydrological responses for what was chosen as a relatively planar hillslope area, identification of a simplified nor even relatively complex physically based hydrological model structure (such as that of *Bronstert* [1999]) would be problematic. The question then is how important is this detail in the representation of responses at the catchment scale and whether general patterns that will not reflect all the local detail will suffice [e.g., *Woods et al.*, 1997].

5.4. The Importance of Bedrock Control at the Catchment Scale, Trench Positioning, and Riparian Linkages

[52] The positioning of the hillslope trench may have affected our results. Had the trench been located some tens of meters upslope, there may not have been enough upslope-accumulated area to generate readily definable mobile flow pathways along the bedrock surface. Had the trench been installed some tens of meters downslope from its present site in the riparian zone around the hillslope–riparian interface, down-valley flow effects may have been observed (as reported recently by *McHale et al.* [2000]). In this downslope position it is likely that water tables may have persisted between rainstorms. These interactions can be complex and alter the chemistry and timing of water arriving at the channel [*McGlynn et al.*, 1999]. This is something that is currently being explored at PMRW. However, what is clear from the measurements is that the hillslope responses at the trench site lag the streamflow responses (Figure 4).

[53] At PMRW, flow from the hillslope contributes to storm flow at the catchment scale. During the largest rainstorm on 6 March, streamflow was generated during the 49 mm rainfall on 6 March, but flow did not occur at the trench until the second major pulse of rain (47 mm) on 7 March (Figure 4). Despite the absence of flow at the trench during the first rainfall pulse, it is likely that hillslope flow further downslope and along the stream channel may have contribute to streamflow. Also, the hillslope contribution increased as the watershed became wetter during the second rainfall pulse. *Burns et al.* [2001] applied an end-member mixing analysis (EMMA) using five major solutes (Na, Mg, Cl, SO_4, and H_4SiO_4) from samples collected of bedrock runoff, hillslope flow (from the trench) and riparian zone groundwater to explain the variations in stream water composition at the subcatchment gage during the 6 March rainstorm. Their analysis suggests that subcatchment streamflow was dominated by the outcrop runoff throughout the rainstorm and as much as 90% during the peak flows. The EMMA analysis suggested that flow from the hillslope contributed, on average, 16% and ranged from 10% to 30% of the subcatchment composition with the maximum contribution occurring during the recession period. Because the outcrop runoff was the dominant contributor to streamflow, it is likely that the overall water yield would be less in catchments that contain less impervious area, i.e., less outcrop area, but that the hillslope contribution to the total streamflow would increase.

[54] Consistent with what we observed at PMRW, *Hinton et al.* [1993] suggest the need for new and improved geophysical techniques to map sediment thickness over large areas. Their results found discrepancies between surface topography and the direction of groundwater flow, noting that hydrological models based on DEMs would be best applied if the surface could be related to groundwater equipotentials (noting that this was a dynamic property depending on flow conditions). Recently catchment modeling at PMRW, which included different landscape units, which represent catchment areas with distinct soil depths including bedrock outcrops, hillslopes and the riparian zone, within the Dynamic TOPMODEL structure, has increased the performance of the model simulations for stream discharge [*Peters et al.*, 2001]. These results are part of our ongoing research at PMRW to assess the need to incorporate subsurface topography in model simulations at the catchment scale.

6. Conclusions

[55] A trenched 20 m wide by 48 m long hillslope on granitic bedrock was surveyed and instrumented at the PMRW, Georgia. Flow from 2 m trench sections and several individual macropores were monitored and augmented with tensiometer data in the hillslope above the trench for three rainstorms on 4 February (60 mm), 6 March (95 mm), and 27 March 1996 (25 mm). Matrix flow occurred from the hillslope during each rainstorm and macropore flow occurred during the larger two rainstorms. Flow was significantly delayed when compared to the rainfall and streamflow from the catchment. The deeper trench sections dominated total subsurface storm flow and peak flow responses and contained the macropores.

[56] A 2 m grid survey of ground surface and bedrock surface elevations of the hillslope was used to produce a detailed map of the two surfaces. Two sets of accumulated upslope area and topographic indices were calculated, one using the ground surface topography ($SURF_{acc}$ and $SURF_{atb}$) and one the surface of an impeding layer associated with the soil–bedrock interface (BR_{acc} and BR_{atb},). An evaluation of the relations between upslope contributing area and flow for "snapshots" during the 6 March rainstorm indicates that bedrock topography controls the trench storm flow response, and that ground surface topography is a poor predictor. Furthermore, the hillslope hydrologic response was directly coupled with the spatial development of the saturated zone as these are also predicted by the spatial patterns of the bedrock derived index

[57] As the hillslope wets up the predictions of the indices improve, thereby supporting the concept of an increasingly connected flow system upslope that is gaining more conformity with the assumptions of the indices. Also, trench flow varies with time, and to some extent the variability in the timings of these flow responses are observed in the different responses in flowpaths upslope of relevant sections. Macropore flow contributes significantly to storm flow, and that the response characteristics of the

macropore flow differ from trench sections dominated by matrix flow.

References

Ambroise, B., J. E. Freer, and K. J. Beven, Application of a generalized TOPMODEL to the small Ringelbach catchment, Vosges, France, *Water Resour. Res.*, *32*, 2147–2159, 1996.

Anderson, S. P., W. E. Dietrich, D. R. Montgomery, R. Torres, M. E. Conrad, and K. Loague, Subsurface flow paths in a steep, unchanneled catchment, *Water Resour. Res.*, *33*, 2637–2653, 1997.

Atkins, R. L., and M. W. Higgins, Superimposed folding and its bearing on geological history of the Atlanta, Georgia area, in *Excursions in South-Eastern Geology, Vol. I, Atlanta Ga.*, edited by R. W. Frey, pp. 19–40, AGU, Washington, D. C., 1980.

Atkinson, T. C., Techniques for measuring subsurface flow on hillslopes, in *Hillslope Hydrology*, edited by M. J. Kirkby, pp. 73–120, John Wiley, New York, 1978.

Barling, R. D., I. D. Moore, and R. B. Grayson, A quasi-dynamic wetness index for characterising the spatial distribution of zones of surface saturation and soil water content, *Water Resour. Res.*, *30*, 1029–1044, 1994.

Beven, K. J., Changing ideas in hydrology: The case of physically-based models, *J. Hydrol.*, *105*, 157–172, 1989a.

Beven K. J., Interflow, in *Unsaturated Flow in Hydrological Modelling—Theory and Practice*, edited by H. J. Morel-Seytoux, pp. 191–219, Kluwer Acad., Norwell, Mass., 1989b.

Beven, K. J., A discussion of distributed hydrological modelling, in *Distributed Hydrological Modelling*, edited by M. B. R. Abbott, pp. 255–278, Kluwer Acad., Norwell, Mass., 1996a.

Beven K. J., Process, heterogeneity and scale in modelling soil moisture fluxes, in *Global Environmental Change and Land Surface Process in Hydrology: The Trials and Tribulations of Modelling and Measuring*, edited by S. Sorooshian, V. K. Gupta, and J. Rodda, pp. 191–214, Springer-Verlag, New York, 1996b.

Beven, K. J., Uniqueness of place and process representations in hydrological modelling, *Hydrol. Earth Syst. Sci.*, *4*, 203–213, 2000.

Beven, K. J., How far can we go in distributed hydrological modelling?, *Hydrol. Earth Syst. Sci.*, *5*, 1–12, 2001.

Beven, K. J., and J. Freer, A dynamic TOPMODEL, *Hydrol. Processes*, *15*, 1993–2011, 2001.

Beven, K. J., and M. J. Kirkby, A physically based, variable contributing area model of basin hydrology, *Hydrol. Sci. Bull.*, *24*, 43–69, 1979.

Bronstert, A., Capabilities and limitations of detailed hillslope hydrological modelling, *Hydrol. Processes*, *13*, 21–48, 1999.

Bunting, B. T., The role of seepage moisture in soil formation, slope development and stream initiation, *Am. J. Sci.*, *259*, 503–519, 1961.

Burns, D. A., R. P. Hooper, J. J. McDonnell, J. E. Freer, C. Kendall, and K. Beven, Base cation concentrations in subsurface flow from a forested hillslope: The role of flushing frequency, *Water Resour. Res.*, *34*, 3535–3544, 1998.

Burns, D. A., J. J. McDonnell, R. P. Hooper, N. E. Peters, J. E. Freer, C. Kendall, and K. Beven, Quantifying contributions to storm runoff through end-member mixing analysis and hydrologic measurements at the Panola Mountain Research Watershed (Georgia, USA), *Hydrol. Processes*, *15*, 903–924, 2001.

Burt, T. P., and D. P. Butcher, Topographic controls of soil moisture distributions, *J. Soil Sci.*, *36*, 469–486, 1985.

Buttle, J. M., and D. S. Turcotte, Runoff processes on a forested slope on the Canadian shield, *Nord. Hydrol.*, *30*, 1–20, 1999.

Carter, M. E. B., A community analysis of the Piedmont deciduous forest of Panola Mountain State Conservation Park, Atlanta, Georgia, unpublished M.S. thesis, Emory Univ., Emory, 1978.

Crave, A., and C. Gascuel-Odoux, The influence of topography on time and space distribution of soil surface water content, *Hydrol. Processes*, *11*, 203–210, 1997.

Dunne, T., and R. D. Black, Partial area contributions to storm runoff in a small New England watershed, *Water Resour. Res.*, *6*, 1296–1311, 1970.

Freer, J., J. McDonnell, K. J. Beven, D. Brammer, D. Burns, R. P. Hooper, and C. Kendal, Topographic controls on subsurface storm flow at the hillslope scale for two hydrologically distinct small catchments, *Hydrol. Processes*, *11*, 1347–1352, 1997.

Genereux, D. P., H. F. Hemond, and P. J. Mulholland, Spatial and temporal variability in streamflow generation on the west fork of Walker Branch Watershed, *J. Hydrol.*, *142*, 137–166, 1993.

Gilman, K., and M. D. Newson, Soil pipes and pipeflow: A hydrological study in upland Wales, in *British Geomorphological Research Group Monograph Series*, p. 114, GeoBooks, Norwich, England, 1980.

Grayson, R. B., I. D. Moore, and T. A. McMahon, Physically based hydrologic modelling, 2, Is the concept realistic?, *Water Resour. Res.*, *26*, 2659–2666, 1992.

Hewlett, J. D., and A. R. Hibbert, Moisture and energy conditions within a sloping soil mass during drainage, *J. Geophys. Res.*, *68*, 1081–1087, 1963.

Hinton, M. J., S. L. Schiff, and M. C. English, Physical-properties governing groundwater-flow in a glacial till catchment, *J. Hydrol.*, *142*, 229–249, 1993.

Hooper, R., B. Aulenbach, D. Burns, J. J. McDonnell, J. Freer, C. Kendall, and K. J. Beven, Riparian control of streamwater chemistry: Implications for hydrochemical basin models, *Int. Assoc. Hydrol. Sci.*, *248*, 451–458, 1998.

Huntington, T. G., R. P. Hooper, N. E. Peters, T. D. Bullen, and C. Kendall, Water, energy and biogeochemical budgets investigations at Panola Mountain Research Watershed, Stockbridge, Georgia: A research plan, *U.S. Geol. Surv. Open File Rep.*, *93-55*, 1993.

Hutchinson, D. G., and R. D. Moore, Throughflow variability on a forested hillslope underlain by compacted glacial till, *Hydrol. Processes*, *14*, 1751–1766, 2000.

Iorgulescu, I., and A. Musy, Generalisation of TOPMODEL for a power law transmissivity profile, *Hydrol. Processes*, *11*, 1353–1355, 1997.

Jones, J. A. A., Some limitations of the a/s index for predicting basin-wide patterns of soil water drainage, *Z. Geomorphol.*, *60*, 7–20, 1986.

Jones, J. A. A., Pipeflow contributing areas and runoff response, *Hydrol. Processes*, *11*, 35–41, 1997.

Jordan, J. P., Spatial and temporal variability of stormflow generation processes on a Swiss catchment, *J. Hydrol.*, *153*, 357–382, 1994.

Kirkby, M., Hydrograph modelling strategies, in *Processes in Physical and Human Geography*, edited by R. Peel et al., pp. 69–90, Heinemann, London, 1975.

Lamb, R., K. Beven, and S. Myrabø, Discharge and water table predictions using a generalized TOPMODEL formulation, *Hydrol. Processes*, *11*, 1145–1167, 1997.

McDonnell, J. J., A rationale for old water discharge through macropores in a steep, humid catchment, *Water Resour. Res.*, *26*, 2821–2832, 1990.

McGlynn, B. L., J. J. McDonnell, J. B. Shanley, and C. Kendall, Riparian zone flowpath dynamics during snowmelt in a small headwater catchment, *J. Hydrol.*, *222*, 75–92, 1999.

McHale, M. R., M. J. Mitchell, J. J. McDonnell, and C. P. Cirmo, Nitrogen solutes in an Adirondack forested watershed: Importance of dissolved organic nitrogen, *Biogeochemistry*, *48*, 165–184, 2000.

McIntosh, J., J. J. McDonnell, and N. E. Peters, Tracer and hydrometric study of preferential flow in large undisturbed soil cores from the Georgia Piedmont, USA, *Hydrol. Processes*, *13*, 139–155, 1999.

Moore, R. D., and J. C. Thompson, Are water table variations in a shallow forest soil consistent with the TOPMODEL concept, *Water Resour. Res.*, *32*, 663–669, 1996.

Nyberg, L., Spatial variability of soil water content in the covered catchment at Gårdsjön, Sweden, *Hydrol. Processes*, *10*, 89–103, 1996.

O'Loughlin, E. M., Saturation regions in catchments and their relations to soil and topographic properties, *J. Hydrol.*, *53*, 229–246, 1981.

Peters, N. E., and E. B. Ratcliffe, Tracing hydrologic pathways using chloride at the Panola Mountain Research Watershed, Georgia, USA, *Water Air Soil Pollut.*, *105*, 263–275, 1998.

Peters N. E., J. Freer, and K. J. Beven, Modeling hydrologic responses in a small forested catchment (Panola Mountain, Georgia, USA)—A comparison of the original and a new dynamic TOPMODEL, *Hydrol. Processes*, in press, 2002.

Quinn, P. F., K. J. Beven, P. Chevallier, and O. Planchon, The prediction of hillslope flow patterns for distributed hydrological modelling using digital terrain models, *Hydrol. Processes*, *5*, 59, 1991.

Ratcliffe, E. B., N. E. Peters, and M. Tranter, Short-term hydrological response of soil water and groundwater to rainstorms in a deciduous forest hillslope, Georgia, USA, in *Advances in Hillslope Processes*, edited by M. G. B. Anderson, pp. 129–147, John Wiley, New York, 1996.

Shanley, J. B., Factors controlling sulphate retention and transport at Panola Mountain, Georgia, unpublished Ph.D. thesis, Univ. of Wyoming, Laramie, Wyo., 1989.

Shanley, J. B., and N. E. Peters, Variations in aqueous sulfate concentrations at Panola Mountain, Georgia, *J. Hydrol.*, *146*, 361–382, 1993.

Sklash, M. G., K. J. Beven, K. Gilman, and G. Darling, Isotope studies of pipeflow at Plynlimon, Wales, UK, *Hydrol. Processes*, *10*, 921–944, 1996.

Tsuboyama, Y., R. C. Sidle, S. Noguchi, and I. Hosoda, Flow and solute transport through the soil matrix and macropores of a hillslope segment, *Water Resour. Res.*, *30*, 879–890, 1994.

Tsukamoto, T., and T. Ohta, Runoff process on a steep forested slope, *J. Hydrol.*, *102*, 165–178, 1988.

Turton, D. J., C. T. Haan, and E. L. Miller, Subsurface flow response of a small forested catchment in the Ouachita mountains, *Hydrol. Processes*, *6*, 111–125, 1992.

Woods, R., and L. Rowe, The changing spatial variability of subsurface flow across a hillside, *J. Hydrol.*, *35*, 51–86, 1996.

Woods, R. A., M. Sivapalan, and J. S. Robinson, Modelling the spatial variability of subsurface runoff using a topographic index, *Water Resour. Res.*, *33*, 1061–1073, 1997.

Zumbuhl, A. T., Spatial modeling of soil depth and landscape variability in a small, forested catchment, unpublished M.S. thesis, Coll. of Environ. Sci. and For., State Univ. of New York, Syracuse, NY, 1998.

———————————

B. Aulenbach and N. E. Peters, U.S. Geological Survey, Atlanta, GA 30360, USA.

K. J. Beven and J. Freer, Department of Environmental Sciences, IENS, University of Lancaster, Lancaster, UK. (j.freer@lancaster.ac.uk)

D. A. Burns, U.S. Geological Survey, Troy, NY 12180, USA.

R. P. Hooper, U.S. Geological Survey, Northborough, MA 01532, USA.

C. Kendall, U.S. Geological Survey, Menlo Park, CA 94025, USA.

J. J. McDonnell, Department of Forest Engineering, Oregon State University, Corvallis, OR, USA.